forests

MDPI

Article

Study of Sawing Parameters for *Caragana korshinskii* (C.K.) Branches

Yaoyao Gao [1,2], Yutong Wang [1], Aili Qu [1], Jiangming Kan [2], Feng Kang [2] and Yutan Wang [1,*]

[1] School of Mechanical Engineering, Ningxia University, Yinchuan 750021, China; gaoyy@bjfu.edu.cn (Y.G.); wangyt6261@126.com (Y.W.); qq_qal@163.com (A.Q.)
[2] School of Technology, Beijing Forestry University, Beijing 100083, China; kanjm@bjfu.edu.cn (J.K.); kangfeng98@bjfu.edu.cn (F.K.)
* Correspondence: wang_yt1108@163.com; Tel.: +86-0951-2062998

Abstract: To solve the problems of poor sawing surface quality, severe blade wear and high power consumption caused by unreasonable working parameters in the process of *Caragana korshinskii* (C.K.) stumping, this study explored the effects of branch diameter (D), sawing speed (v_c), feeding speed (v_f), cutting inclination (α), number of circular saw teeth (T) and moisture content (M) on sawing power consumption (P) and sawing surface quality (A) through a single-factor test using a homemade branch sawing bench. Based on the Box–Behnken design principle, a multi-factor test was carried out based on a single-factor test with v_c, v_f, α and T as influencing factors and with P and A as targets, establishing a regression model. The test results show that the sawing power consumption (P) increases with increasing D, decreases with increasing M, and decreases first and then increases with increasing v_c, v_f, α and T; the sawing surface quality (A) increases first and then decreases with increasing D, increases with increasing M, and first increases and then decreases with increasing v_c, v_f, α and T. The optimum combination of parameters for the regression model was obtained with v_c of 45.24 m/s, v_f of 0.34 m/s, α of 10° and T of 100, which resulted in the P of 177.46 J and A of 85.87%. The errors between the predicted and actual values of P and A are 3.1% and 6%, respectively. The study can provide information to support the development of subsequent C.K. stubble equipment.

Keywords: *Caragana korshinskii* branches; sawing test bench; mechanization; sawing parameters; optimization; influencing factors

check for updates

Citation: Gao, Y.; Wang, Y.; Qu, A.; Kan, J.; Kang, F.; Wang, Y. Study of Sawing Parameters for *Caragana korshinskii* (C.K.) Branches. *Forests* **2022**, *13*, 327. https://doi.org/10.3390/f13020327

Academic Editor: Milan Gaff

Received: 10 January 2022
Accepted: 15 February 2022
Published: 17 February 2022

Publisher's Note: MDPI stays neutral with regard to jurisdictional claims in published maps and institutional affiliations.

Copyright: © 2022 by the authors. Licensee MDPI, Basel, Switzerland. This article is an open access article distributed under the terms and conditions of the Creative Commons Attribution (CC BY) license (https://creativecommons.org/licenses/by/4.0/).

1. Introduction

Caragana korshinskii (C.K.), as one of the most important plants for sand fixation, can improve desertification in Western China [1–3], and plays an important role in the management of desertification of China [4,5]. C.K. not only has an important ecological effect but also has higher economic benefits [6]. Stubble rejuvenation is an important measure in the management of sandy shrubs during their growth and is the key to the healthy and sustainable development of shrubbery forests [7]. Depending on the growth characteristics of C.K., the branches need to be stumped once every 3–5 years, otherwise its growth slows down and even dies naturally [8]. At present, the main harvesting method of C.K. is manual cutting or using backpack cutters for stubble harvesting, which is inefficient, labor heavy and damaging to the body [9]. As the planted area continues to expand, relying on manual cutting cannot meet production requirements, and the need for mechanized stubble harvesting equipment is becoming increasingly urgent. Exploring the performance parameters of the C.K. branches is of significant importance to the development of stubble equipment.

The cutter is one of the key components of the C.K. stubble equipment and has a direct impact on the cutting quality and the cutting efficiency of the branches. Currently, there are three major types of cutters widely used in agricultural and forestry harvesters: reciprocating, chain-sawing and circular sawing [10–12]. The following conclusions were

reached through comparative analysis: (1) Reciprocating cutters have higher cutting efficiency and are widely used in wheat harvesters and grass cutters [13,14]. As C.K. grows in an arid desert environment, the branch cutting resistance is high and the cutter is seriously damaged during the working process, which makes its application in sandy shrub stubble operation greatly restricted. (2) Chain-sawing cutters are mainly used in operational environments such as tree delimbing and forest harvesting [15,16]. The C.K. roots are full of leaves, which often block the chain-sawing cutter and prevent it from operating properly. (3) The circular sawing cutter has a higher cutting efficiency. If the appropriate sawing parameters are selected, the circular saw is more stable in its working and has a higher cutting quality [17,18]. In addition, the circular sawing cutter is relatively simple in construction and makes it easier to automate the stubbing of the C.K. branches. Therefore, we use a circular saw as the cutting tool.

Current research on the cutting characteristics of stems of agroforestry plants is focused on the following. For example, Zhang, Y. et al. [19] conducted response surface tests with average cutting speed, cutting angle and blade bevel angle as factors to optimize cutting parameters for grain stalk cutting and to reduce the cutting power consumption of the cutter. Cui, Y.J et al. [20] studied the effects of blade distance, sliding cutting angle, bevel cutting angle and shear angle on shear stress by using a shear fixture on a universal testing machine to investigate the optimal combination of parameters for harvesting hydroponic lettuce with a reciprocating cutter. Kang, F et al. [21] took apple branches as the research object and simulated the actual cutting conditions in the field indoors to analyze the effects of average cutting speed, cutting gap and slip cutting angle on the peak cutting force and to provide a theoretical basis for the subsequent prototype. Wargula, L. et al. [22] analyzed the cutting power consumption of four different commonly used wood shredding mechanisms: disc, drum, double-cylinder and flail, under the same conditions. Abdallah, R. et al. [23] explored the influencing factors affecting log cutting forces and constructed a model of cutting patterns during slicing by installing a cutting force measurement device on a cutting test bench. Vu, V.D. et al. [24] used corn straw with 81% moisture content as the object of study and used response surface methodology to explore the effects of tool front angle, feed angle and cutting speed on cutting force and power consumption, and the optimized straw grinder could reduce cutting force and power consumption by 2.3 times and 4 times, respectively. Mathanker, S.K. et al. [25] used a self-designed high-speed stalk cutting test bench to cut sugarcane stalks and found that the cutting power consumption of sugarcane stalks increased with increasing cutting speed, and that choosing a larger blade bevel angle instead made the cutting power consumption of sugarcane stalks higher.

Many scholars have performed extensive research on the cutting mechanism of circular saws and on improving the sawing surface quality. Fekiac, J. et al. [26] explored the effects of feed rate, cutting speed and average chip thickness on the energy consumption and surface temperature of circular saw blades, using plywood of 14 mm thickness as the sawing target. S. Turchetta et al. [27] retrofitted a CNC machining center with a force gauge and data acquisition system to measure and evaluate the cutting forces at different stages of operation. It was found that the cutting forces of diamond discs cutting granite decreased with increasing cutting speed and increased with increasing feed per revolution. Jozef Krilek et al. [17] used two circular saw blades with different tooth pitches to test sawing spruce and pine trees, respectively. It was found that the irregular tooth pitch circular saws consumed more energy than the regular tooth pitch circular saws, with a linear increase in energy consumption with increasing feed speed. Orlowski, K. et al. [28] used an improved cutting model to predict the cutting state of Pinus sylvestris. The results showed that the root means square error of the cutting power obtained with the improved model was slightly greater than the experimental value. Wang, K.D. et al. [29] established a chip geometry model to derive the relationship between chip diameter and chip arc length regarding the average chip thickness. The aim is to reveal the mechanism of wear differences and provide a theoretical basis for the optimization of circular saws. Ján Svoren et al. [30] used a non-contact infrared transducer to monitor the cutting en-

ergy and surface temperature of the saw blade to find the optimum conditions for an energy-efficient cutting process to achieve a high-quality surface. Orlowski, K.A. et al. [31] took images of the serrations using a NIKON ECLIPSE Ti-S microscope, analyzed the serrations in the image software and measured the length of the cutting edge. Wen-Tung Chang et al. [32] conducted cutting tests on workpieces using alloy steel circular saws to develop response surface models and evaluate the main factors affecting machined surface roughness. Weiguang Li et al. [33] investigated the effect of cutting parameters on surface roughness by varying the parameters of the circular saw.

In short, research into the power consumption and surface cut quality of circular saws has focused on wood paneling, stone and metal materials. Relatively few studies have been carried out on the sawing of C.K. and other stalk species. The cutting performance parameters of agroforestry crops, which grow in different environments and vary in physical parameters between species, cannot be directly transferred for use, so independent cutting performance tests were carried out on the C.K. branches.

Therefore, based on a homemade sawing test bench, this paper establishes a multivariate mathematical regression model to optimize the cutting parameters based on the wood cutting principle, using the Box–Behnken central combination test method, with sawing speed, feeding speed, cutting inclination and number of teeth as test factors and sawing power and sawing surface quality score values as objective functions. This study provides parametric support for the improvement and optimization of the C.K. stumping equipment.

2. Test Materials and Equipment

2.1. Test Material

The test materials were sampled in Yanchi County, Ningxia District, China (38°6′21″ N, 106°52′29″ E), in October 2021. The selected branches were basically straight, with continuous and uniform variation in diameter, free of pests and diseases, free of branch nodes, with a diameter range of 8 to 24 mm and a length of 220 mm. After collection, the branches were placed in a thermostat for storage.

2.2. Sawing Test Bench

The experiments were carried out using a self-designed and manufactured sawing test bench, as shown in Figure 1. The cutting test stand consists of 3 parts: the sawing system, the branch feeding system and the measurement and control system.

The sawing system consists of an AC motor, frequency converter, torque sensor JN-DN3, rotary cutting shaft and circular saw blade. The circular saw blade is driven by an AC motor, which is controlled by the inverter to control the speed. The branch feeding system is divided into two parts: the power transmission unit and the branch fixing and adjustment unit. The relative position of the branch and the disc saw blade is adjusted using a ball screw mechanism driven by a servo motor. The posture of the branch is adjusted through the angle adjustment fixture. The measurement and control system consists of the MCC-1608FS-PLUS data acquisition card, the instrument display, the 24 V DC stabilized voltage supply and the Laptop.

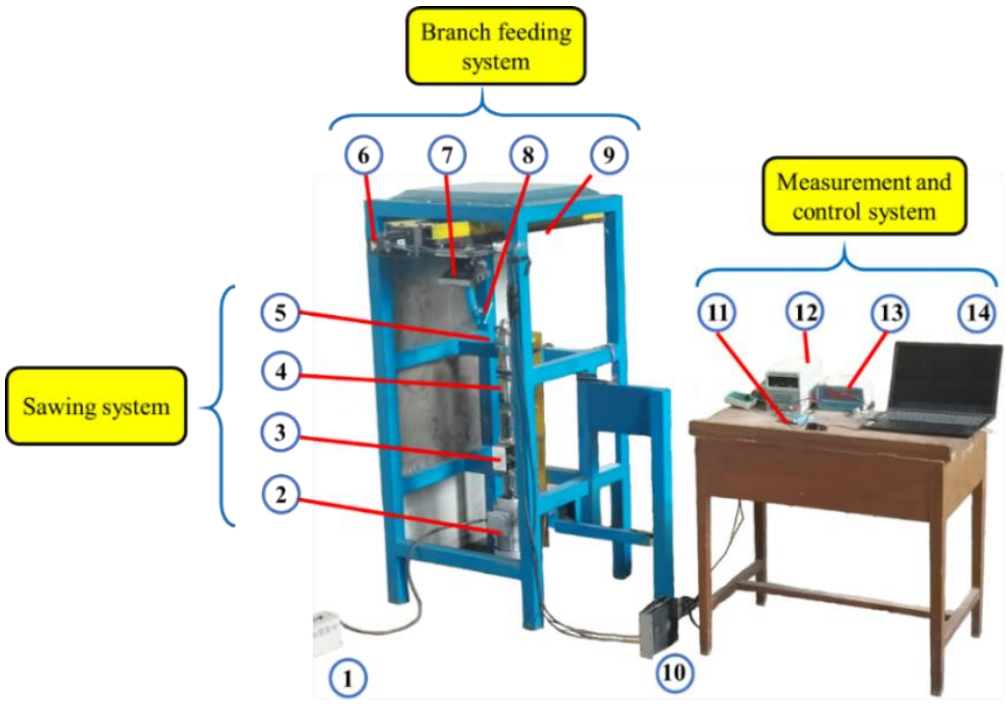


Figure 1. Schematic diagram of the structure of the sawing test bench. (1. Variable-frequency drive 2. AC motor 3. Torque sensor 4. Rotary cutting shafts 5. Circular saw 6. Servo motor 7. Angle adjustment fixture 8. Branch holder 9. Ball screw mechanism 10. Servo drives 11. Data acquisition card 12. Stabilized voltage supply 13. Instrument display 14. Laptop).

3. Test Index

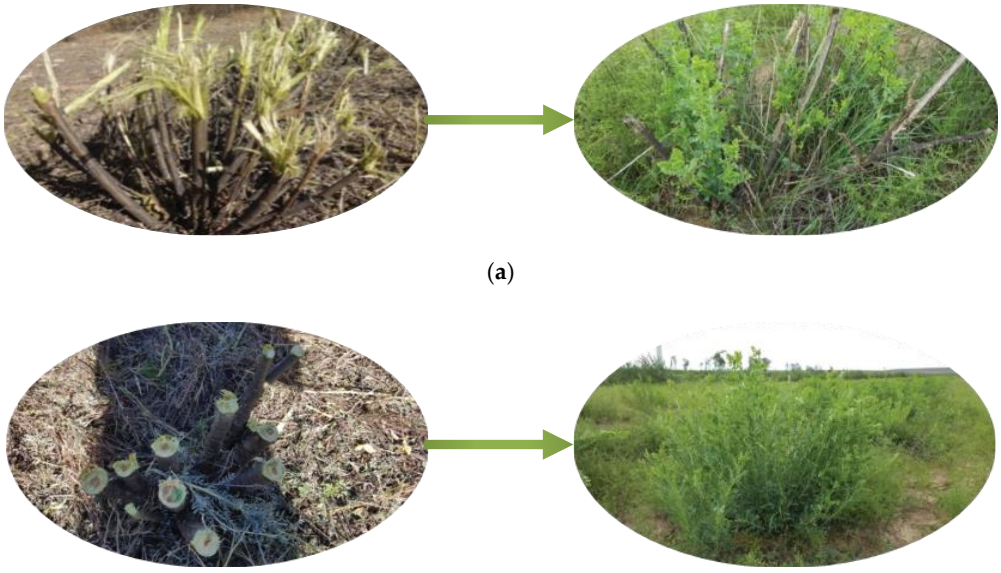
3.1. Test Indicators

1. During crop harvesting operations, energy consumption is an important parameter in the structural design of the harvester to match the power source, which is of great importance in promoting the light weight of the C.K. harvesting equipment and extending the working time of the harvester [22,34]. In this paper, the torque signal from the torque sensor is recorded in real time during the cutting process using an acquisition card, and the sawing power consumption of the branch is obtained by processing the torque signal [35] (Equation (1)).

$$P = \omega \cdot \int M\,(t)dt \tag{1}$$

where: P is the sawing power consumption, J; ω is the angular speed of rotation of the cutting rotation shaft, rad/s; $M(t)$ is the curve of the torque sensor as a function of time; t is the time variable, s.

2. According to the biological characteristics and agronomic requirements of C.K., the stubble must be smooth and flat when cutting branches, without burning or tearing. If the surface of the cross-section is torn, water is easily dissipated and can easily result in low germination rates or even death of the plant the following year [8,36,37]. The survey found a higher germination rate with flat cross-sections than with burr cross-sections, as shown in Figure 2.



(**a**)

(**b**)

Figure 2. Stubble cross-sections of C.K. and germination rate the following year ((**a**) Burr cross-section germination rate in the following year; (**b**) Flat cross-sections germination rate in the following year).

To facilitate analysis and measurement, the sawing quality of the cross-section (broken area as a percentage of the area of the branch cross-section) is determined using the broken area ratio τ [38,39]. The area of the branch cross-section as well as the area of the damaged part was extracted by Matlab software, as shown in Figure 3.



(**a**) (**b**) (**c**)

Figure 3. Extraction of branch cross-sectional area((**a**) Original image; (**b**) Extraction of branch cross-section; (**c**) Extraction of damaged parts).

The sawing surface quality A can be obtained as follows:

$$\tau = \frac{A_1}{A_2} \tag{2}$$

$$A = 1 - \tau \times 100\% \tag{3}$$

where: A is t sawing surface quality score, %; A_2 is the cross-sectional area of the branch, mm^2; A_1 is the area of the damaged section, mm^2.

3.2. Test Factors

As shown in Figure 4, the sawing force F can be equated to a radial force F_n, a tangential force F_t and an axial force F_a, with α being the cutting inclination of the circular saw [40,41], in which the radial force F_n mainly comes from the impact of the branches on the disc saw during sawing. The tangential force F_t is mainly generated by the friction between the surface of the disc saw and the cutting surface of the branches during sawing. The axial

force F_a is mainly caused by the machining errors of the circular saw and the extrusion of the branches on the circular saw. The axial force F_a of the circular saw is decomposed into a vertical downward force F_z and a horizontal force F_{x1}, where F_z, F_{x1} can be expressed as follows:

$$F_z = F_a \cdot cos\alpha \tag{4}$$

$$F_{x1} = F_a \cdot sin\alpha \tag{5}$$

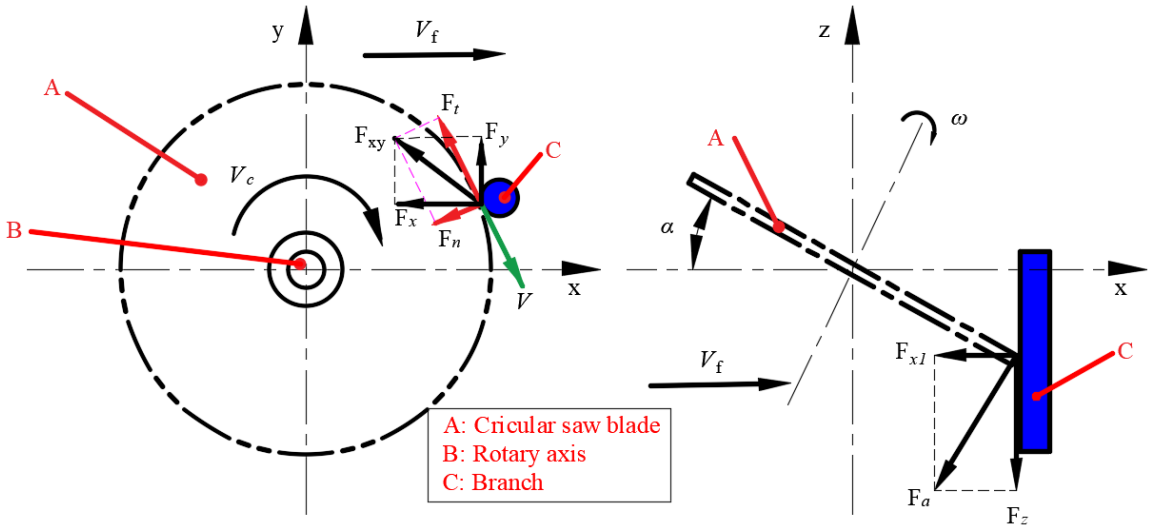


Figure 4. Diagram of cutting forces on saw blades.

When sawing branches, the combined force on the circular saw can be written as follows:

$$F = \sqrt{(F_{x1} + F_x)^2 + F_n^2 + F_t^2} \tag{6}$$

The feed rate is proportional to the feed speed and inversely proportional to the cutting speed and number of serrations. The feed per tooth is written as follows:

$$S = \frac{S_n}{Z} = \frac{60 \times V_f}{V_c \times Z} \tag{7}$$

$$v_c = \frac{\pi D n}{6 \times 10^4} \tag{8}$$

where: S is the feed per tooth of the circular saw, mm; S_n is the feed per revolution of the circular saw, mm; Z is the number of teeth; V_f is the feeding speed, m/s; V_c is the sawing speed, m/s; n is the motor rotation speed, r/min.

According to Equations (4)–(8), the cutting speed, feeding speed, cutting inclination and number of teeth are important factors affecting the power consumption of the saw blade and the quality of the cutting surface during the sawing process.

In summary, branch diameter, sawing speed, feeding speed, cutting inclination and number of circular saw teeth were selected as test factors. The frequency converter controls the sawing speed of the circular saw. The servo motor drives the ball screw mechanism and controls the feeding speed of the branches. Concerning domestic and foreign stubble tools, manganese steel saw blades have the advantages of high-cost performance and good wear resistance [23,41]. Therefore, manganese steel saw blades of the same diameter with different numbers of teeth are selected as cutting tools. The cutting inclination of the branch of the circular saw is adjusted by using the angle adjustment fixture, the structure of which is shown in Figure 5.

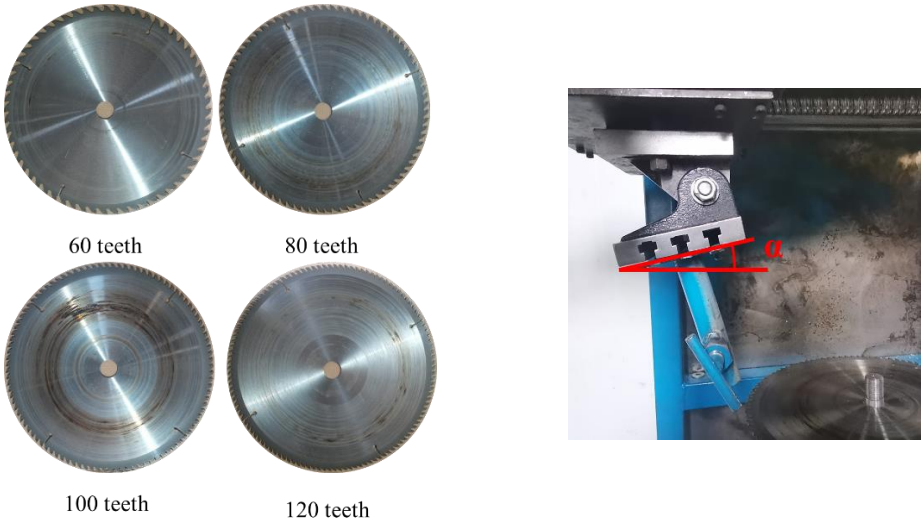


Figure 5. Cutting parameters ((**a**) Number of blade teeth; (**b**) Cutting inclination).

4. Experimental Design

4.1. Single-Factor Experimental Design

In summary, a total of six single-factor tests were designed for branch diameter D, sawing speed V_c, feeding speed V_f, cutting inclination α, number of teeth T and moisture content M, using power consumption P and cut surface quality score A as target values. The factors and levels of the single-factor test are shown in Table 1. During the C.K. stubble cycle, most branches do not generally exceed 16 mm in diameter [8], so for a more complete study of the relationship between the branch and cutting power, the diameter D was taken to be 6–20 mm in the single-factor test and 10–12 mm in the other groups when carried out. When the sawing speed is higher, there is a risk of test operation, so the sawing speed is taken as 20–50 m/s in the single-factor test of sawing speed and 40 m/s when conducting other groups of single-factor experiments. The feeding speed is selected from 0.15 to 0.55 m/s concerning the operating speed of the forage harvester and 0.35 m/s when conducting other groups of trials [42,43]. Concerning other scholars [40,44], the cutting inclination is set to 0–20° in the cutting inclination singular factor test, and 10° is chosen for the cutting inclination when conducting other groups of tests. According to the agronomic requirements of C.K., it is usually required to retain stubble at a height of no more than 10 cm from the ground to facilitate branch sprouting [8,38]. However, the sandy and gravelly environment in which C.K. grows makes it easy to wear out the tools when the cutting height becomes low. Therefore, the cutting height is set to 5 cm. Each test is repeated five times.

Table 1. Factors and levels of the single-factor test.

Level	Branch Diameter D (mm)	Sawing Speed V_c (m/s)	Feeding Speed V_f (m/s)	Cutting Inclination α (°)	Moisture Content M (%)	Number of Teeth T
1	6	20	0.15	0	12.5	60
2	8	25	0.25	5	19.6	80
3	10	30	0.35	10	23.5	100
4	12	35	0.45	15	28.6	120
5	14	40	0.55	20		
6	16	45				
7	18	50				
8	20					

4.2. Multi-Factor Experimental Design

Based on the single factor, a 4-factor, 3-level multi-factor test is designed based on the Box–Behnken principle with sawing speed, feeding speed, cutting inclination and number of teeth as factors (Table 2) and each test is repeated five times. The branches are 10 to 12 mm in diameter and have moisture content of 22.5 to 29.1%.

Table 2. Factors and levels of the multi-factor test.

Level	Sawing Speed V_c (m/s)	Feeding Speed V_f (m/s)	Cutting Inclination α (°)	Number of Teeth T
−1	40	0.25	5	80
0	45	0.35	10	100
1	50	0.45	15	120

5. Results

5.1. Single-Factor Test Results

As shown in Figures 6–11, the sawing power consumption increases sharply with the increase of branch diameter. With the increase of sawing speed, feeding speed, number of teeth and cutting inclination, the sawing power consumption shows a trend of decreasing first and then increasing. With the increase of moisture content, the sawing power consumption gradually decreases.

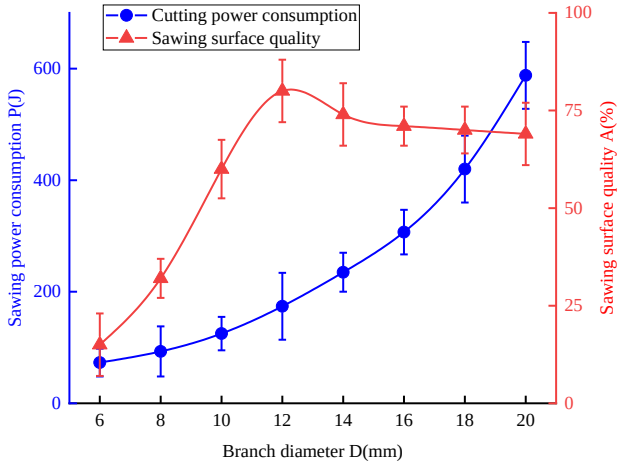


Figure 6. Sawing effect with different branch diameters (Note: Sawing speed 40 m/s; feeding speed 0.35 m/s; cutting inclination 10°; number of teeth 80; moisture content 26.6~28.4%).

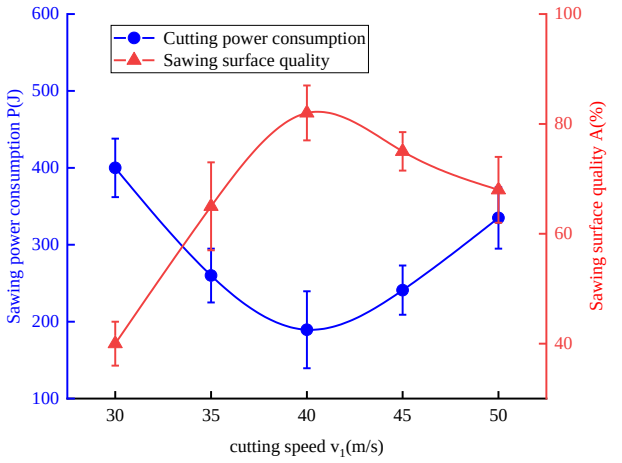


Figure 7. Sawing effect with different sawing speeds (Note: Branch diameter 10~12 mm; feeding speed 0.35 m/s; cutting inclination 10°; number of teeth 80; moisture content 24.7~28.3%).

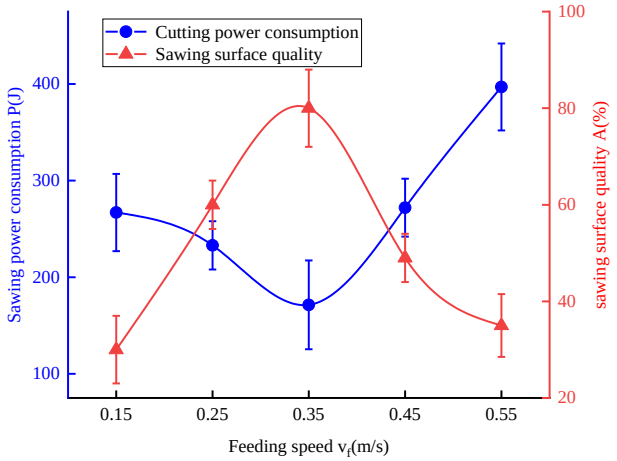


Figure 8. Sawing effect with different feeding speeds (Note: Branch diameter 10~12 mm; sawing speed 40 m/s; cutting inclination 10°; number of teeth 80; moisture content 24.7~28.3%).

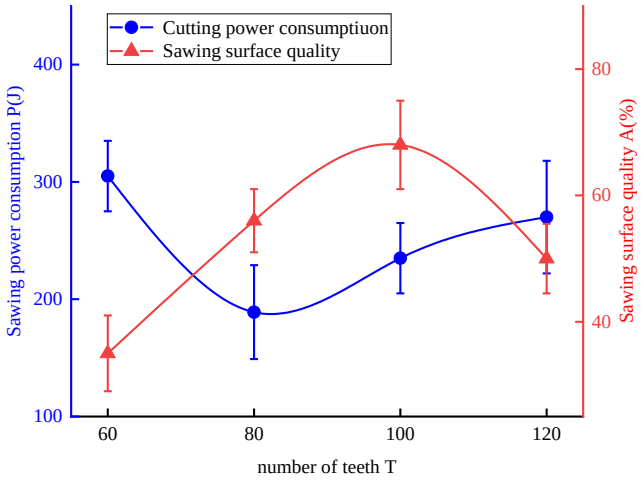


Figure 9. Sawing effect with different numbers of teeth (Note: Branch diameter 10~12 mm; sawing speed 40 m/s; cutting inclination 10°; feeding speed 0.35 m/s; moisture content 25.0~29.9%).

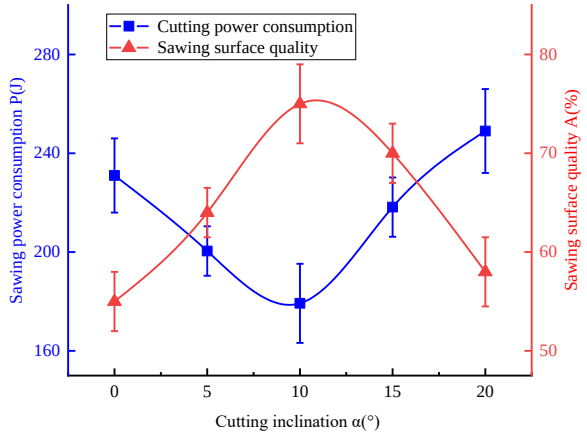


Figure 10. Sawing effect with the different cutting inclination (Note: Branch diameter 10~12 mm; sawing speed 40 m/s; feeding speed 0.35 m/s; number of teeth 80; moisture content 25.0~29.9%).

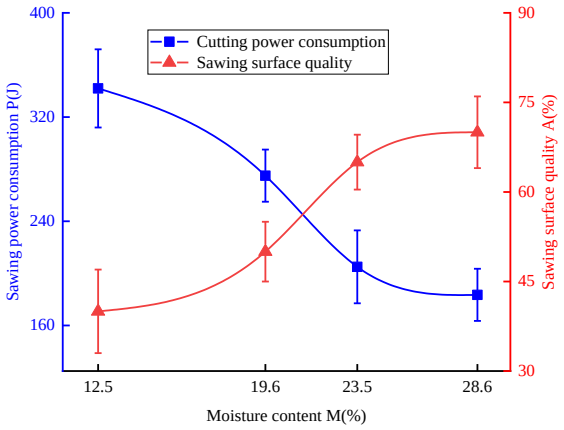


Figure 11. Sawing performance with different moisture contents (Note: Branch diameter 10–12 mm; sawing speed 40 m/s; feeding speed 0.35 m/s; number of teeth 80; cutting inclination 10°).

The sawing surface quality increases and then decrease as the branch diameter increases, and the decreasing trend becomes slower. With the increase of sawing speed, feeding speed, number of teeth and cutting inclination, the sawing surface quality tends to decrease and then increase. With the increase of moisture content, the sawing surface quality gradually increases.

5.2. Multi-Factor Test Results

The experiments were carried out in random order with 24 experimental points and 5 central points according to the Box–Behnken principle to minimize interference with the experiment through external factors. The test was repeated five times for each level to obtain the mean value. The test results are shown in Table 3.

Table 3. Sawing test design scheme and response results.

Level	Sawing Speed V_c (m/s)	Feeding Speed V_f (m/s)	Cutting Inclination α (°)	Number of Teeth T	Sawing Power Consumption P (J)	Sawing Surface Quality A (%)
1	0	0	0	0	188	90
2	1	1	0	0	340.2	46
3	−1	−1	0	0	295.2	48
4	0	−1	−1	0	239.4	58
5	0	0	−1	1	207.3	63
6	0	0	0	0	182.2	83
7	0	0	1	−1	230.6	64
8	0	1	1	0	285.0	45
9	0	−1	0	−1	270.7	42
10	−1	0	0	−1	254.5	50
11	−1	0	−1	0	259.8	60
12	0	1	0	1	269.6	42
13	1	0	0	−1	265.7	64
14	0	0	0	0	175.2	86
15	1	0	−1	0	273.9	61
16	0	0	0	0	166.6	83
17	0	−1	1	0	270.9	63
18	0	0	1	1	224.4	72
19	0	1	−1	0	256.0	48
20	−1	0	0	1	253.4	52

Table 3. *Cont.*

Level	Sawing Speed V_c (m/s)	Feeding Speed V_f (m/s)	Cutting Inclination α (°)	Number of Teeth T	Sawing Power Consumption P (J)	Sawing Surface Quality A (%)
21	1	0	0	1	273.5	71
22	−1	0	1	0	265.6	64
23	0	−1	0	1	240.5	61
24	0	0	−1	−1	217.3	60
25	0	0	0	0	176.8	84
26	1	−1	0	0	275.8	54
27	1	0	1	0	270.1	69
28	−1	1	0	0	299.5	40
29	0	1	0	−1	279.0	46

6. Discussion

6.1. Single-Factor Test Analysis

6.1.1. Branch Diameter

As shown in Figure 6, as the diameter of the branch increases, more cellulose is cut and the sawing power increases significantly [21,45]. Under the same working conditions, a larger cross-sectional area increases the friction and cutting resistance between the saw blade and the branch, making it difficult to feed the branch. Sawing is unsupported cutting. When the branch diameter is smaller, the branch has poor bending resistance and is directly torn by the saw teeth during the cutting process, therefore its cutting surface quality is poor.

The forces on the branch during sawing are shown in Figure 12. The circular saw exerts a cutting force P on the branch during sawing. The following equation can be obtained for a circular saw during smooth cutting.

$$\begin{cases} P = P' \\ T = P \cdot h \end{cases} \tag{9}$$

where: T is the bending moment of the branch, N/m; P is the sawing force of the saw teeth on the branch during sawing, N; h is the vertical distance between the sawing point and the fixed point of the branch, m; and P' is the horizontal force of the fixed support on the branch, N.

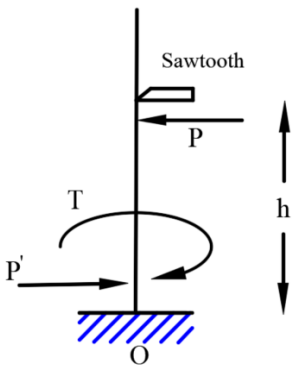


Figure 12. Schematic diagram of the forces on the branch sawing.

During the actual cutting process, the branch receives external forces that deform it in deflection, the size of which depends on the bending resistance of the branch. When the diameter of the branch is smaller, its bending resistance is poor and bending occurs during the cutting process, making the circular saw blade unevenly stressed during the cutting

process, and tearing phenomenon occurs [41,46]. When the branch diameter is larger, the cutting forces can be balanced, and the cutting surface is flatter without tearing (Figure 13).



Figure 13. The surface quality of sawing for different diameters.

6.1.2. Sawing Speed

When the sawing speed is less than 35 m/s, the power consumption of sawing will increase significantly, because at the same feeding speed, the lower sawing speed will increase the sawing volume of a single tooth, and the frictional resistance between the saw blade and the branch increases, so that the power consumption of sawing increases and the surface quality of sawing becomes poor. Due to the existence of certain processing and installation errors, when the sawing speed is greater than 45 m/s, it is easy to cause axial vibration of the saw blade, reducing the stability of the saw blade when working, making the cutting power consumption increase, the sawing surface quality poor [47], and the cross-sectional burning phenomenon occur, as shown in Figure 14.



Figure 14. Sawing surface quality with different sawing speeds ((**a**) $V_c < 35$ m/s; (**b**) $V_c > 45$ m/s).

6.1.3. Feeding Speed

When the feeding speed is less than 0.25 m/s, the branch is repeatedly sawn and the friction between the saw blade and the cross-section increases, which makes the sawing power consumption increase and the sawing surface is burnt. When the feeding speed is greater than 0.45 m/s, the advancing speed of the saw blade is greater than the cutting distance of the saw teeth, and there is an obvious tearing phenomenon of the finished branch being cut, which makes the power consumption according to cutting increase [26], as shown in Figure 15.

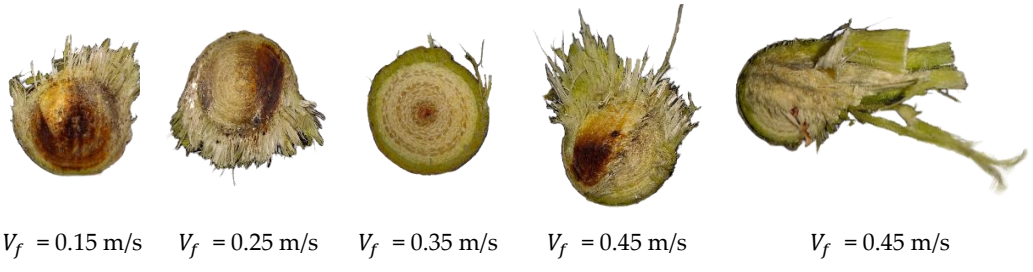


Figure 15. Cutting quality with different feed speeds.

6.1.4. Cutting Inclination

When other working conditions are the same, a larger cutting inclination of the saw blade will lead to a larger area of the non-working surface of the disc saw in contact with the branch, so that the frictional resistance between the disc blade and the branch increases, and the axial force increases significantly, causing axial vibration and deformation of the blade, resulting in a significant increase in sawing power consumption and a decrease in surface cutting quality [48]. However, when the cutting inclination of the circular saw is too small, although the sawing power consumption will be reduced, the bending moment of the branch increases (Equation (13)) and it tends to break from the roots. Therefore, to ensure better cutting quality, the angle of inclination should not be chosen too large or too small.

As shown in Figure 16, during the branch feeding process, the branch is subjected to the cutting force of the circular saw and the angle between the cutting surface and the branch is α. The bending moment equation for the branch can be obtained as follows:

$$M = P{\cdot}b{\cdot}cos\alpha \tag{10}$$

Bending moment stress at the root of a branch is:

$$\sigma = \frac{M}{W} = \frac{P{\cdot}b{\cdot}cos\alpha}{W} \tag{11}$$

where: P is the sawing force of the saw teeth on the branch during sawing, N; α is the cutting inclination, °; and W is the flexural section factor.

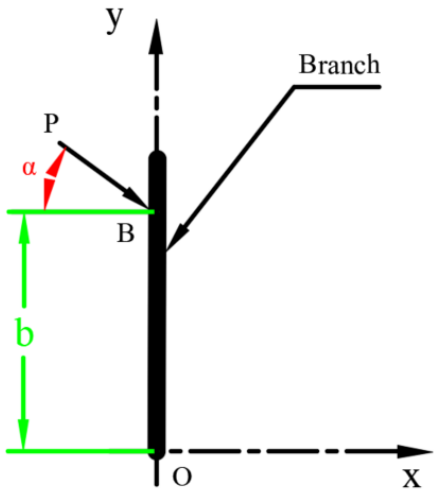


Figure 16. Schematic diagram of the forces on the branches.

6.1.5. Number of Teeth

Under the same parameters, the number of teeth is smaller and the cutting volume per tooth of the saw blade is larger. Thus, it increases the sawing power consumption and makes the sawing surface quality worse. When the number of teeth is excessive, the gap between the teeth is smaller, sawing wood chips are easy to accumulate in the gap between the teeth, and the friction between the saw teeth and the surface of the branch increases, which leads to the increased power consumption of sawing and poor cutting surface quality [49].

6.1.6. Moisture Content

The average moisture content of fresh branches is 28.6%. After the branches were left for 2, 7 and 15 days, the average moisture content of the branches was measured to be

23.5%, 19.6% and 12.5%, respectively, and the four groups of moisture-content branches were tested for sawing.

The sawing power consumption decreases with increasing branch moisture content, and the sawing surface quality score value increases with increasing branch moisture content during the cutting process. As the moisture content of the branches decreases and the dry matter increases, their ultimate stress increases [8,21]. It is recommended that C.K. should be cut in a season when the moisture content of the branches is higher.

6.2. Multi-Factor Test Analysis

6.2.1. Analysis of Variance (ANOVA)

From the ANOVA of the sawing power consumption P in Table 4, it can be seen that the main order of the effects of factors and factor interactions on sawing power consumption is v_c^2, v_f^2, α^2, T^2, v_f, $v_c \cdot v_f$, α, v_c, T, $v_f \cdot T$, $v_c \cdot \alpha$, $v_c \cdot T$, $\alpha \cdot T$, $v_f \cdot \alpha$; where v_c^2, v_f^2, α^2, T^2, v_f, $v_c \cdot v_f$ have a highly significant effect ($p < 0.01$); α, v_c have a significant effect ($0.01 < p \leq 0.05$), and the other effects are not significant ($p > 0.05$). The loss of fit term, $p = 0.3435$, is not significant, which means that there are no other major factors affecting the test indicators.

Table 4. Analysis of variance for sawing power consumption.

Variance Source	Sum of Squares	Degree of Freedom	Mean Square	*F* Values	*p* Values
Model	47,917.67	14	3422.69	37.26	<0.0001
v_c	422.45	1	422.45	4.60	0.050 *
v_f	1559.52	1	1559.52	16.98	0.0010 **
α	719.20	1	719.20	7.83	0.0142 *
T	200.90	1	200.90	2.19	0.1613
$v_c \cdot v_f$	903.00	1	903.00	9.83	0.0073 **
$v_c \cdot \alpha$	23.04	1	23.04	0.2508	0.6243
$v_c \cdot T$	19.80	1	19.80	0.2156	0.6496
$v_f \cdot \alpha$	1.56	1	1.56	0.0170	0.8981
$v_f \cdot T$	108.16	1	108.16	1.18	0.2962
$\alpha \cdot T$	3.61	1	3.61	0.0393	0.8457
v_c^2	26,381.48	1	26,381.48	287.23	<0.0001 **
v_f^2	25,825.98	1	25,825.98	281.18	<0.0001 **
α^2	3405.05	1	3405.05	37.07	<0.0001 **
T^2	2911.62	1	2911.62	31.70	<0.0001 **
Residual	1285.87	14	91.85		
Lack of Fit	1029.28	10	102.93	1.60	0.3435
Pure Error	256.59	4	64.15		
Cor Total	49,203.54	28			

Note: $p < 0.01$ (highly significant, **); $p < 0.05$ (significant, *).

The test results are analyzed using Design-expert 11.0 software, and multiple regression fitting of each test index is carried out to remove insignificant factors and obtain the regression equation for each factor level on sawing power as follows:

$$P = 5.93\ v_c + 11.4\ v_f + 7.74\ \alpha - 4.0\ T + 15.03\ v_c \cdot v_f + 63.77\ + 63.10\ v_f^2 + 22.91\ \alpha^2 + 21.19\ T^2 + 177.76 \quad (12)$$

Table 5 shows the ANOVA for the sawn surface quality score values, A. For the sawn surface quality score values, the main order of influence is v_f^2, v_c^2, T^2, α^2, v_f, v_c, $v_f \cdot T$, T, α, $v_f \cdot \alpha$, $\alpha \cdot T$, $v_c \cdot T$, $v_c \cdot \alpha$, $v_c \cdot v_f$, with the effects of v_f^2, v_c^2, T^2, α^2, v_f, v_c, $v_f \cdot T$ being highly significant ($p < 0.01$), T being significant ($0.01 < p \leq 0.05$), and the effects of the other factors not significant ($p > 0.05$). The failure to fit term, $p = 0.3106$, is not significant, indicating that there are no other factors affecting the test indicators.

The experimental results are analyzed using Design-expert 11.0 software and multiple regression fitting of each test index is carried out to remove non-significant factors to

obtain the regression equation for each factor level on the sawn surface quality score values as follows:

$$A = 4.25v_c - 4.92\ v_f + 2.25\ \alpha + 2.92\ T - 5.75\ v_f \cdot T - 13.68\ v_c^2 - 24.43\ v_f^2 - 7.68\ \alpha^2 - 12.68\ T^2 + 85.20 \quad (13)$$

Table 5. Analysis of variance for sawing surface quality score values.

Variance Source	Sum of Squares	Degree of Freedom	Mean Square	*F* Values	*p* Values
Model	5565.03	14	397.50	29.76	<0.0001
v_c	216.75	1	216.75	16.23	0.0012 **
v_f	290.08	1	290.08	21.72	0.0004 **
α	60.75	1	60.75	4.55	0.0511
T	102.08	1	102.08	7.64	0.0152 *
$v_c \cdot v_f$	9.095×10^{-13}	1	9.095×10^{-13}	6.810×10^{-14}	1.0000
$v_c \cdot \alpha$	4.00	1	4.00	0.2995	0.5928
$v_c \cdot T$	6.25	1	6.25	0.4680	0.5051
$v_f \cdot \alpha$	16.00	1	16.00	1.20	0.2922
$v_f \cdot T$	132.25	1	132.25	9.90	0.0071 **
$\alpha \cdot T$	6.25	1	6.25	0.4680	0.5051
v_c^2	1214.49	1	1214.49	90.94	<0.0001 **
v_f^2	3872.35	1	3872.35	289.96	<0.0001 **
α^2	382.92	1	382.92	28.67	0.0001 **
T^2	1043.46	1	1043.46	78.13	<0.0001 **
Residual	186.97	14	13.35		
Lack of Fit	152.17	10	15.22	1.75	0.3106
Pure Error	34.80	4	8.70		
Cor Total	5752.00	28			

Note: $p < 0.01$ (highly significant, **); $p < 0.05$ (significant, *).

6.2.2. Response Surface Analysis

As shown in Figure 17, the effect of feeding speed on sawing power consumption is more significant, and the trend of change in the response surface is consistent with the results of the regression equation analysis in Table 3. The overall effect regulation between the factors is that sawing power consumption with the increase of sawing speed, feeding speed, cutting inclination, and number of teeth, showed a trend of first decreasing and then increasing, consistent with the conclusion of the single-factor test.

As shown in Figure 18, the trend in the response surface of the sawing surface quality is consistent with the results of the ANOVA regression equation in Table 4, and the overall effect of the factors is that the sawing surface quality score tends to increase and then decrease with increasing sawing speed, feeding speed, cutting inclination and number of teeth. The main reason is that when the sawing speed is low, feeding speed is high and the number of teeth is less, the forward speed of the saw blade is greater than the cutting distance of the saw teeth, and on the cut branches appears an obvious tearing phenomenon. When the sawing speed is high, feed speed is low and the number of teeth is more, the saw blade and the surface of the branch produce useless friction work, which produces the phenomenon of burns.

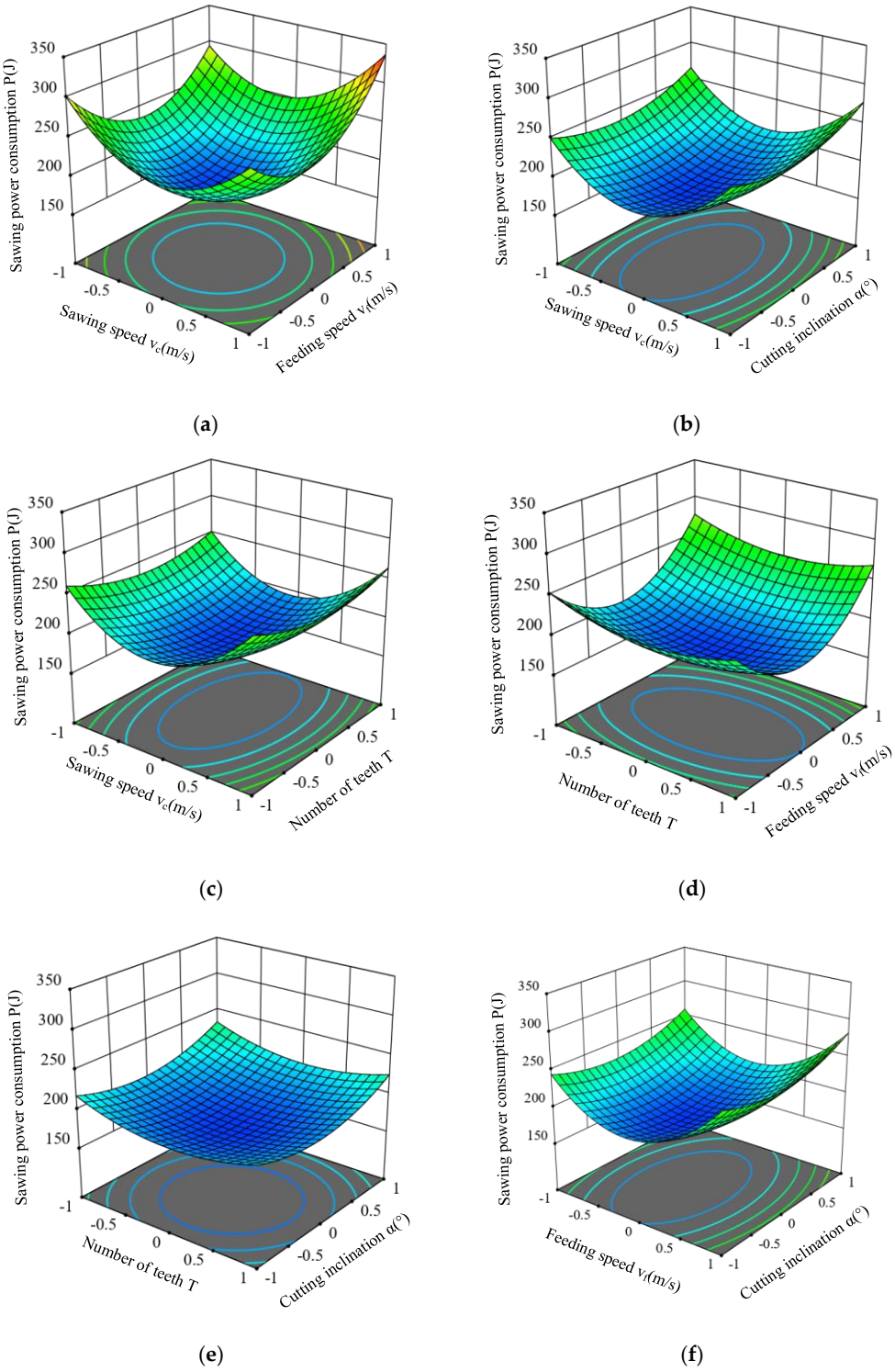


Figure 17. The influence of interaction factors on sawing power consumption. ((**a**) P = f(v_c,v_f,0,0); (**b**) t = f(v_c,0, α,0); (**c**) P = f(v_c,0,0,T); (**d**) P = f(0,v_f,0,T); (**e**) P = f(0,0,α,T); (**f**) P = f(0,v_f,α,T)).

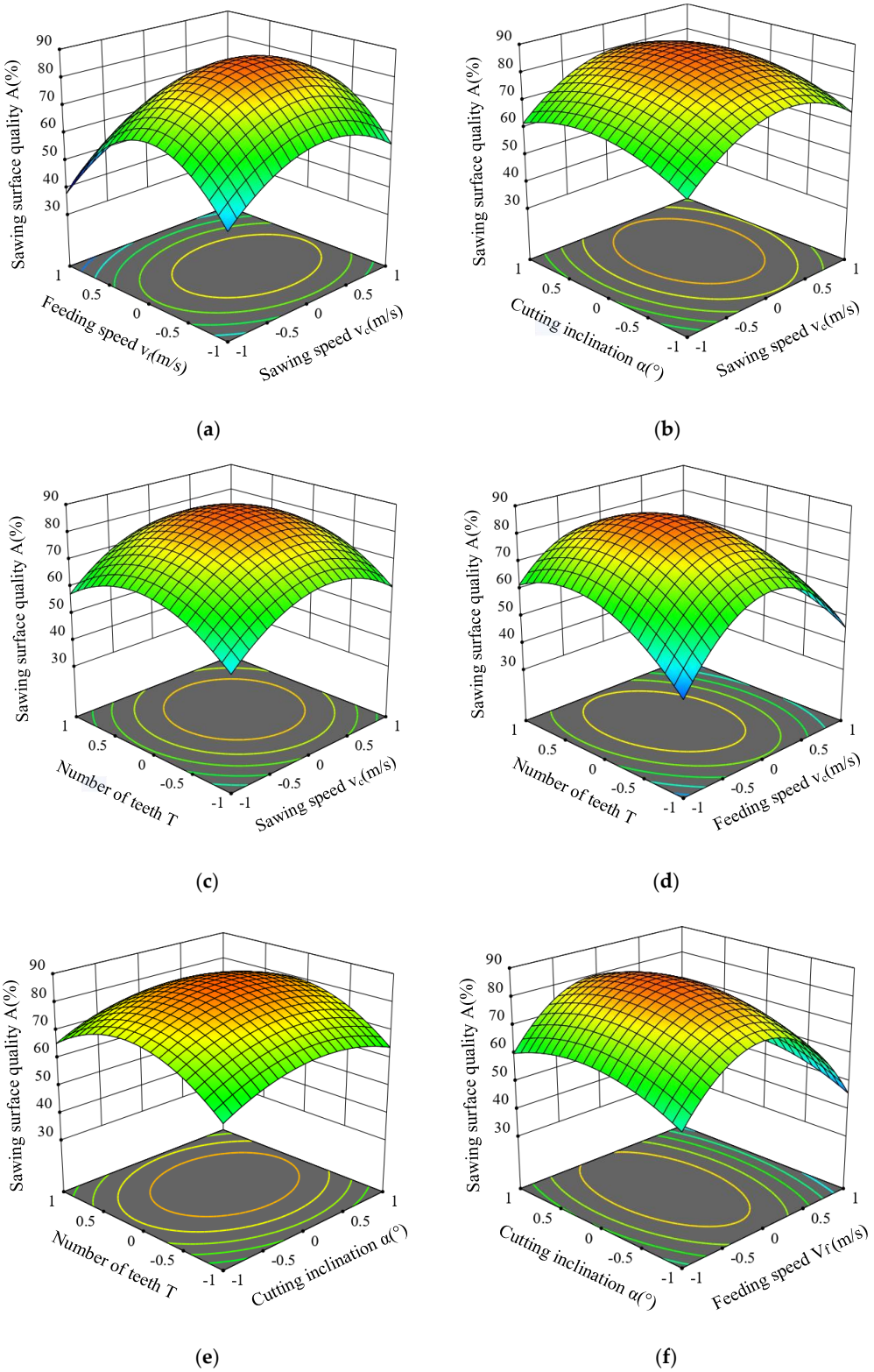


Figure 18. Influence of interaction factors on sawing surface quality. ((**a**) A = f(v_c,v_f,0,0); (**b**) A = f(v_c,0, α,0); (**c**) A = f(v_c,0,0,T); (**d**) A = f(0,v_f,0,T); (**e**) A = f(0,0,α,T); (**f**) A = f(0,v_f,α,T)).

6.3. Parameter Optimization and Experimental Validation

To obtain the best combination of performance parameters for the sawing parameters of the C.K. branches, the minimum value of the sawing power consumption and the maximum value of the sawing surface quality score are taken as the optimization objectives.

Based on the actual working conditions and the analysis results, the conditions for the optimal solution were obtained as follows:

$$\begin{cases} 40\ \text{m/s} \le v_c \le 50\ \text{m/s} \\ 0.25\ \text{m/s} \le v_f \le 0.45\ \text{m/s} \\ 5^\circ \le \alpha \le 15^\circ \\ 80 \le T \le 120 \\ minP = f_1\left(v_c, v_f, \alpha, T\right) \\ maxA = f_2\left(v_c, v_f, \alpha, T\right) \end{cases} \quad (14)$$

By optimizing the solution, the sawing speed is 45.24 m/s, the feeding speed is 0.34 m/s, the cutting inclination is 10° and the number of teeth is 100, the sawing power consumption is 177.46 J, and the sawing surface cut quality score is 85.87%.

Based on the optimal parameters, it was obtained from the response surface experimental optimization analysis that the average sawing power consumption measured on the sawing test bench was 183.03 J and the average sawing surface quality score was 80.6%, with an error value of 3.1% and 6%, respectively, from the predicted value (Table 6).

Table 6. Analysis of variance for sawing surface quality score values.

Test Serial Number	Sawing Power Consumption *P* (J)	Sawing Surface Quality *A* (%)
1	170.5	83
2	182.7	80
3	195.9	79
Average value	183.03	80.6
Relative errors	3.1%	6%

7. Conclusions

(a) The sawing power consumption and sawing surface quality in the process of C.K. branch sawing were tested by a self-designed branch sawing test bench. The relationship between branch diameter, sawing speed, feeding speed, cutting inclination, number of teeth, moisture content and sawing power consumption and sawing surface quality were explored through single-factor tests. Tests result: ① Sawing power consumption increases with increasing branch diameter, but decreases with increasing moisture content. With increasing sawing speed, feeding speed, cutting inclination and number of teeth, the power consumption decreases and then increases. ② The sawing surface quality score increases and then decreases with increasing branch diameter, but increases with increasing moisture content. With increasing sawing speed, feeding speed, cutting inclination and number of teeth on the saw blade, the sawing surface quality score increases and then decreases.

(b) The effects of the factors on the target values coincided with the single-factor test, and the optimal combination of parameters in the test range is as follows: sawing speed is 45.24 m/s, feeding speed is 0.34 m/s, cutting inclination is 10° and number of teeth is 100. When sawing the C.K. branches with a diameter of 10–12 mm, the sawing power consumption for this combination is 183.03 J and the sawing surface cut quality score is 80.6. The errors between the predicted sawing power consumption and sawing surface score values of the model obtained from the multi-factor test and the actual values are 3.1% and 6%, respectively.

(c) The factors of the branch sawing device have a significant influence on the sawing power consumption in the order of feeding speed, sawing speed, cutting inclination and number of teeth. The factors of the branch sawing device have a significant influence on the sawing surface quality in the order of feeding speed, number of teeth, sawing speed and cutting inclination.

(d) The experimental parameters of the sawing test bench are closer to the actual operating environment than the finite element simulation, and the estimated sawing power consumption and the optimal combination of parameters are more in line with the actual situation, which can provide data support for the subsequent development of high-efficiency harvesting equipment.

Author Contributions: Conceptualization, Y.W. (Yutan Wang) and F.K.; methodology, Y.G.; software, A.Q.; validation, Y.G., Y.W. (Yutong Wang) and J.K.; formal analysis, F.K.; investigation, A.Q.; resources, J.K.; data curation, Y.W. (Yutong Wang); writing—review and editing, Y.G.; visualization, Y.W. (Yutong Wang); supervision, J.K.; project administration, Y.W. (Yutan Wang). All authors have read and agreed to the published version of the manuscript.

Funding: This research was funded by NingXia key research and development program (Grant No. 2019BBF02009).

Institutional Review Board Statement: Not applicable.

Informed Consent Statement: Not applicable.

Data Availability Statement: Test methods and data are available from the authors upon request.

Acknowledgments: Sincere thank also goes to Junrui Xue for his kind help in manuscript reviewing and drawing design.

Conflicts of Interest: The authors declare no conflict of interest.

References

1. Xu, H.; Wang, Z.J.; Li, Y.; He, J.L.; Wu, X.D. Dynamic growth models for Caragana korshinskii shrub biomass in China. *J. Environ. Manag.* **2020**, *269*, 13. [CrossRef] [PubMed]
2. Long, Y.; Liang, F.P.; Zhang, J.W.; Xue, M.D.; Zhang, T.B.; Pei, X.W. Identification of drought response genes by digital gene expression (DGE) analysis in Caragana korshinskii Kom. *Gene* **2020**, *725*, 8. [CrossRef] [PubMed]
3. Li, W.C.; Zhang, S.J.; Zhang, T.Z.; Shen, Y.Q.; Han, L.J.; Peng, Z.J.; Xie, Z.X.; Zhong, C.; Jia, S.R. Bacterial cellulose production from ethylenediamine pretreated Caragana korshinskii Kom. *Ind. Crop. Prod.* **2021**, *164*, 10. [CrossRef]
4. Liang, H.B.; Xue, Y.Y.; Shi, J.W.; Li, Z.S.; Liu, G.H.; Fu, B.J. Soil moisture dynamics under Caragana korshinskii shrubs of different ages in Wuzhai County on the Loess Plateau, China. Earth Environ. *Sci. Trans. R. Soc. Edinb.* **2019**, *109*, 387–396. [CrossRef]
5. Roy, R.; Mostofa, M.G.; Wang, J.X.; Fornara, D.; Sarker, T.; Zhang, R.Q. Revegetation intervention of drought-prone coal-mined spoils using Caragana korshinskii under variable water and nitrogen-phosphorus resources. *Agric. Water Manag.* **2021**, *246*, 12. [CrossRef]
6. Zhang, J.; Zheng, D.C.; Wu, K.; Zhang, X.Q. Combustion Characteristics of Caragana korshinskii Kom. *J. Biobased Mater. Bioenergy* **2019**, *13*, 69–78. [CrossRef]
7. Wang, Y.; Zhao, H.L.; Zhao, X.Y. Effects of land use intensity on the restoration capacity of sandy land vegetation and soil moisture in fenced sandy land in desert area. *Contemp. Probl. Ecol.* **2013**, *6*, 128–136. [CrossRef]
8. Gao, Y.Y.; Kang, F.; Kan, J.M.; Wang, Y.T.; Tong, S.Y. Analysis and experiment of cutting mechanical parameters for Caragana korshinskii (C.K.) Branches. *Forests* **2021**, *12*, 1359. [CrossRef]
9. Guo, Y.F.; Qi, W. Correlations between Roots of Caragana korshinskii and Soil Moisture after Stumping. *Ekoloji* **2018**, *27*, 9–20.
10. Momin, M.A.; Wempe, P.A.; Grift, T.E.; Hansen, A.C. Effects of four base cutter blade designs on sugarcane stem cut quality. *Trans. Asabe* **2017**, *60*, 1551–1560. [CrossRef]
11. Sahoo, A.U.; Raheman, H. Development of an electric reaper: A clean harvesting machine for cereal crops. *Clean Technol. Environ. Policy* **2020**, *22*, 955–964. [CrossRef]
12. Han, Y.; Xiao, H.R.; Song, Z.Y.; Ding, W.Q. Design and evaluation of tea-plucking machine for improving quality of tea. *Appl. Eng. Agric.* **2019**, *35*, 979–986. [CrossRef]
13. Rafiq, M.H.; Ahmad, R.; Jabbar, A.; Munir, H.; Hussain, M. Influence of different no-till techniques at varying heights of standing rice stubbles on the wheat performance. *Int. J. Agric. Biol.* **2017**, *19*, 410–416. [CrossRef]
14. Aponte-Roa, D.A.; Collazo, X.; Goenaga, M.; Espinoza, A.A.; Vazquez, K. Development and Evaluation of a Remote Controlled Electric Lawn Mower. In Proceedings of the 9th IEEE Annual Computing and Communication Workshop and Conference (CCWC), Las Vegas, NV, USA, 7–9 January 2019; pp. 90–94.
15. Kumar, S.; Dinesha, P.; Rosen, M.A. Performance and emission characteristics of a bio-lubricated two-stroke gasoline engine. *Environ. Sci. Pollut. Res.* **2018**, *25*, 17789–17796. [CrossRef] [PubMed]
16. Romoli, L. Cutting force monitoring of chain saw machines at the variation of the rake angle. *Int. J. Rock Mech. Min. Sci.* **2018**, *101*, 33–40. [CrossRef]

17. Krilek, J.; Tavodova, M.; Kovac, J.; Tichy, B. Impact of irregular tooth pitch of circular saw blades on power for wood cross-cutting. *Drv. Ind.* **2020**, *71*, 3–11. [CrossRef]
18. Huang, G.Q.; Zhang, M.Q.; Huang, H.; Guo, H.; Xu, X.P. Estimation of power consumption in the circular sawing of stone based on tangential force distribution. *Rock Mech. Rock Eng.* **2018**, *51*, 1249–1261. [CrossRef]
19. Zhang, Y.; Cui, Q.; Guo, Y.; Li, H. Experiment and analysis of cutting mechanical properties of millet stem. *Nongye Jixie Xuebao/Trans. Chin. Soc. Agric. Mach.* **2019**, *50*, 146–155. [CrossRef]
20. Cui, Y.J.; Wang, W.Q.; Wang, M.H.; Ma, Y.D.; Fu, L.S. Effects of cutter parameters on shearing stress for lettuce harvesting using a specially developed fixture. *Int. J. Agric. Biol. Eng.* **2021**, *14*, 152–158. [CrossRef]
21. Kang, F.; Tong, S.; Zhang, H.; Li, W.; Chen, Z.; Zheng, Y. Analysis and experiments of reciprocating cutting parameters for apple tree branches. *Nongye Gongcheng Xuebao/Trans. Chin. Soc. Agric. Eng.* **2020**, *36*, 9–16. [CrossRef]
22. Wargula, L.; Kukla, M.; Wieczorek, B.; Krawiec, P. Energy consumption of the wood size reduction processes with employment of a low-power machines with various cutting mechanisms. *Renew. Energy* **2022**, *181*, 630–639. [CrossRef]
23. Abdallah, R.; Auchet, S.; Meausoone, P.J. A dynamic measurement of a disc chipper cutting forces. *Biomass Bioenerg.* **2014**, *64*, 269–275. [CrossRef]
24. Vu, V.D.; Ngo, Q.H.; Nguyen, T.T.; Nguyen, H.C.; Nguyen, Q.T.; Nguyen, V.D. Multi-objective optimisation of cutting force and cutting power in chopping agricultural residues. *Biosyst. Eng.* **2020**, *191*, 107–115. [CrossRef]
25. Mathanker, S.K.; Hansen, A.C. Impact of miscanthus yield on harvesting cost and fuel consumption. *Biomass Bioenerg.* **2015**, *81*, 162–166. [CrossRef]
26. Fekiac, J.; Svoren, J.; Gaborik, J.; Nemec, M. Reducing the energy consumption of circular saws in the cutting process of plywood. *Coatings* **2022**, *12*, 55. [CrossRef]
27. Turchetta, S.; Sorrentino, L. Forces and wear in high-speed machining of granite by circular sawing. *Diam. Relat. Mat.* **2019**, *100*, 8. [CrossRef]
28. Orlowski, K.; Ochrymiuk, T. A newly-developed model for predicting cutting power during wood sawing with circular saw blades. *Maderas-Cienc. Tecnol.* **2017**, *19*, 149–162. [CrossRef]
29. Wang, K.D.; Zhou, J.G.; Zhang, J.S.; Zhang, H.; Cao, T.Y.; Wang, J.K.; Zhao, T.Y. Investigation of diamond wear characteristics of combination saw during granite cutting based on the chip geometry. *Diam. Relat. Mat.* **2021**, *119*, 9. [CrossRef]
30. Svoreň, J.; Naščák, Ľ.; Barcík, Š.; Koleda, P.; Stehlík, Š. Influence of circular saw blade design on reducing energy consumption of a circular saw in the cutting process. *Appl. Sci.* **2022**, *12*, 1276. [CrossRef]
31. Orlowski, K.A.; Chuchala, D.; Przybylinski, T.; Legutko, S. Recovering evaluation of narrow-kerf teeth of mini sash gang saws. *Materials* **2021**, *14*, 7459. [CrossRef]
32. Chang, W.T.; Chen, L.C. Design and experimental evaluation of a circular saw blade with self-clamped cutting inserts. *Int. J. Adv. Manuf. Technol.* **2016**, *83*, 365–379. [CrossRef]
33. Li, W.G.; Zhang, Z.K.; Peng, X.R.; Li, B. The influences of circular saws with sawteeth of mic-zero-degree radial clearance angles on surface roughness in wood rip sawing. *Ann. For. Sci.* **2017**, *74*, 9. [CrossRef]
34. Huang, J.C.; Tian, K.P.; Shen, C.; Zhang, B.; Liu, H.L.; Chen, Q.M.; Li, X.W.; Ji, A.M. Design and parameters optimization for cutting-conveying mechanism of ramie combine harvester. *Int. J. Agric. Biol. Eng.* **2020**, *13*, 94–103. [CrossRef]
35. Shen, C.; Zhang, B.; Li, X.W.; Yin, G.D.; Chen, Q.M.; Xia, C.H. Bench cutting tests and analysis for harvesting hemp stalk. *Int. J. Agric. Biol. Eng.* **2017**, *10*, 56–67. [CrossRef]
36. Huang, J.C.; Shen, C.; Ji, A.M.; Tian, K.P.; Zhang, B.; Li, X.W.; Chen, Q.M. Design and test of two-wheeled walking hemp harvester. *Int. J. Agric. Biol. Eng.* **2020**, *13*, 127–137. [CrossRef]
37. Pei, Z.; Duan, G.; Hao, S.; Qiao, J.; Qin, W. Optimization of stumping method based on wind control benefit for Salix psammophila shrub in Mu Us sandy land. *Nongye Gongcheng Xuebao/Trans. Chin. Soc. Agric. Eng.* **2019**, *35*, 153–161. [CrossRef]
38. Liu, Z.; Ma, Z.; Sui, G.; Zou, D.; Li, G. Optimization design and reliability analysis of salix cutting tools based on finite element method. *Int. J. Perform. Eng.* **2019**, *15*, 441. [CrossRef]
39. Ma, Y.; Xu, C.; Cui, Y.; Fu, L.; Liu, H.; Yang, C. Design and test of harvester for whole hydroponic lettuce with low damage. *Nongye Jixie Xuebao/Trans. Chin. Soc. Agric. Mach.* **2019**, *50*, 162–169. [CrossRef]
40. Hou, J.M.; Bai, J.B.; Yao, E.C.; Zhu, H.J. Design and parameter optimization of disc type cutting device for castor stem. *IEEE Access* **2020**, *8*, 191152–191162. [CrossRef]
41. Meng, Y.M.; Wei, J.D.; Wei, J.; Chen, H.; Cui, Y.S. An ANSYS/LS-DYNA simulation and experimental study of circular saw blade cutting system of mulberry cutting machine. *Comput. Electron. Agric.* **2019**, *157*, 38–48. [CrossRef]
42. Wu, B.; Wang, D.; Wang, G.; Fu, Z.; Kang, C. Optimization and experiments of cut-condition device working parameter on mower conditioner. *Nongye Jixie Xuebao/Trans. Chin. Soc. Agric. Mach.* **2017**, *48*, 76–83. [CrossRef]
43. Zhu, L.; Wang, D.; You, Y.; Wu, B.; Ma, W.; Huan, X. Design and experiment of crawler-type grass belt harvester in forest. *Nongye Jixie Xuebao/Trans. Chin. Soc. Agric. Mach.* **2021**, *52*, 126–133. [CrossRef]
44. Gupta, C.P.; Lwin, L.; Kiatiwat, T. Development of a self-propelled single-axle sugarcane harvester. *Appl. Eng. Agric.* **1996**, *12*, 427–434. [CrossRef]
45. Wang, Y.; Zhang, Y.T.; Yang, Y.; Zhao, H.M.; Yang, C.H.; He, Y.; Wang, K.; Liu, D.; Xu, H.B. Discrete element modelling of citrus fruit stalks and its verification. *Biosyst. Eng.* **2020**, *200*, 400–414. [CrossRef]

46. Alam, M.T.; Kinoshita, N.; Tanaka, C.; Yoshinobu, M. Circular saw lateral stability by optimization of feed speed. *Holz Als Roh-Und Werkst.* **2002**, *60*, 207–209. [CrossRef]
47. Nasir, V.; Mohammadpanah, A.; Cool, J. The effect of rotation speed on the power consumption and cutting accuracy of guided circular saw: Experimental measurement and analysis of saw critical and flutter speeds. *Wood Mater. Sci. Eng.* **2020**, *15*, 140–146. [CrossRef]
48. Tian, J.F.; Hutton, S.G. Cutting-induced vibration in circular saws. *J. Sound Vibr.* **2001**, *242*, 907–922. [CrossRef]
49. Mello, R.D.C.; Harris, H. Cane damage and mass losses for conventional and serrated basecutter blades. In Proceedings of the 2000 Conference of the Australian Society of Sugar Cane Technologists Held at Bundaberg, Bundaberg, Australia, 2–5 May 2000; pp. 84–91.